Rotary motor powered by stochastic uncorrelated dipoles

Cheng-Hung Chang[1,2] and Tian Yow Tsong[3,4,*]
[1]*Physics Division, National Center for Theoretical Sciences, Hsinchu 300, Taiwan*
[2]*Institute of Physics, National Chiao Tung University, Hsinchu 300, Taiwan*
[3]*Institute of Physics, Academy of Sciences, Taipei 115, Taiwan*
[4]*National Chiao-Tung University and National Nanodevice Laboratory, Hsinchu 300, Taiwan*
(Received 9 May 2005; revised manuscript received 19 July 2005; published 1 November 2005)

It is demonstrated that the stochastic back-and-forth vibrations of uncorrelated dipoles may lead to rotation of their ambient dipoles. This peculiar phenomenon is clarified by considering spatial and temporal symmetry breakings. The former asymmetry is the result of the multiple biased Hamiltonian vector fields, which is a ratchet effect, and the latter, of the time sequence specified by a metastable state. Since this driving mechanism is simpler than that of F_0F_1ATPase, it could benefit the design of nanometer scale rotary devices.

DOI: 10.1103/PhysRevE.72.051901 PACS number(s): 87.15.Aa, 05.40.−a, 87.15.He

I. INTRODUCTION

The ratchet mechanism has gained considerable currency recently ranging over different disciplines. Examples include myosin heads in muscles [1], ion pumps on the cell membrane [2–5], Luttinger liquids in solid state physics [6], vortices in Josephson junction arrays [7], cold atoms in an optical lattice [8], magnetic flux quanta [9], and granular systems [10,11]. In this respect, Smoluchowski's gedanken experiment presents a starting point [12]: can a microscopic device consisting of a wheel with asymmetric sawteeth linked to a pawl harvest kinetic energy from the randomly bombarding air molecules? The device would have satisfied the attribute of perpetual motion and the second law of thermodynamics would have been violated. Feymann extracted an important lesson from this device [13]. The device may indeed harvest energy from a nonequilibrium noise if a spatial asymmetry is built into it. Here we consider a molecular size dipole ratchet that possesses the attributes of the Feymann ratchet and examine the symmetry or symmetry breaking that is required for the device to work as intended. The dipole ratchet model (DRM) proposed verifies many concepts of Feymann and provides some general principles for the design of nanometer scale rotary motors, a subbranch of motor research attracting increasing attention recently [14–19].

As an example, suppose a dipole fixed on a rotor disk is surrounded by three driver dipoles like those in Fig. 1. The drivers can only vibrate stochastically back and forth between two orientations, while the rotor can rotate to any orientation. When the stochastic orientational fluctuation is generated on these uncorrelated drivers, the rotor disk will begin to rotate. Plotting the potential function of the whole system with respect to the rotor angle θ, we shall see later that this rotation is because the phase point $(\theta, \dot{\theta})$ of the rotor is randomly switched between eight Hamiltonian vector fields which have spatially asymmetric attractors in their basins. In other words, the underlying mechanism for the unidirectional rotation of the DRM is a ratchet effect. In conventional ratchets, the stochastic force (random noise) usually appears directly in the single stochastic dynamics of some state variable, like θ, which characterizes the system state. Nevertheless, the stochastic force on the drivers in the DRM plays a different role, which switches the state variable stochastically between several deterministic dynamics. Both kinds of ratchets have stochastic dynamics, but are driven in different ways. The DRM provides an apparent system capable of creating order from disorder and extracting energy from stochastic forces to perform directional motion.

Further, we show that the spatial symmetry breaking in the ratchet effect can generate a directional rotation in the DRM with $N \geqslant 2$ drivers; however, it fails if the driver number is one, i.e., $N=1$. But a further study shows a directional rotation is still possible for $N=1$, if this driver has an additional metastable state between the original two states. Mathematically it is at first glance a bit puzzling how a back-and-forth dynamics, which has a singularity at the turning points, can be mapped into a smooth rotational dynamics without

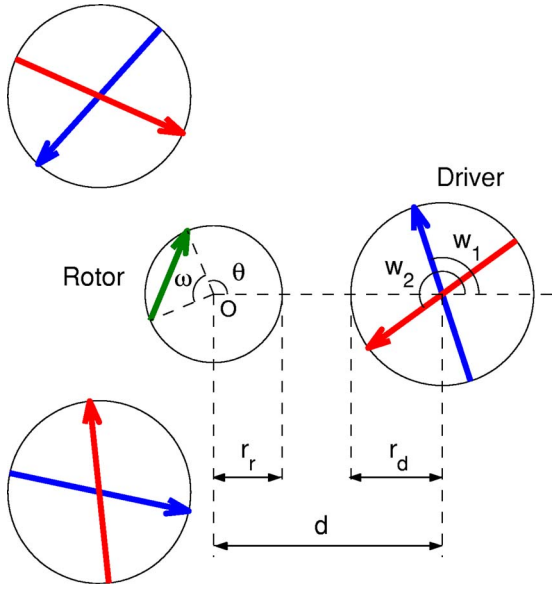

FIG. 1. (Color online) Dipole ratchet with three drivers, every one of which has two conformational states with orientations w_1 and w_2.

 ©2005 The American Physical Society

turning points through a smooth transformation like the Coulomb interaction. The reason is that the sequential change between this metastable state and the other two original states specifies a rotation direction on a circle, giving a temporal symmetry breaking to the system.

Two advantages of the DRM enhance the realization probability of fabricating a nanoscale artificial rotary motors. First, a force transduction through the dipole interaction is less sensitive to the motor shape and to the surrounding thermal fluctuations, compared with that through a hard surface contact like sawtooth wheels. Second, driving a motor with stochastic uncorrelated drivers is simpler than that with correlated drivers. In the extreme case when the vibrations of the three drivers in Fig. 1 are correlated, the system setup is closer to the function mechanism of the biological motor F_0F_1ATPase [20]. The efficiencies, common features, and advantages of the DRM and F_0F_1ATPase are compared.

II. DIPOLE RATCHET MODEL

The DRM studied here consists of a central rotor surrounded by N uniformly separated drivers. Figure 1 is an example for $N=3$, which mimics the structure of the three pairs of α and β proteins on the F_1 motor of F_0F_1ATPase [21]. The effective dipoles of the inhomogeneously distributed charges are represented by the vectors shown. While the rotor can rotate to an arbitrary angle, only two orientations w_1 and w_2 are allowed for the drivers, corresponding to low and high energy conformational states. The driver state can be changed, for instance, by the high energy bound of ATP. If an ATP molecule is associated with a driver and hydrolyzed, an amount of energy is released to the driver, which then favors staying at the high energy state. After the energy is exhausted, the driver tends to come back to the low energy state. While the ATP arrives at each driver stochastically, its docking and energy release after hydrolysis can be either stochastic or periodic on each driver. The former (latter) corresponds to a uncorrelated (correlated) driving.

The motion of the rotor orientation θ can be described by the equation,

$$J\ddot{\theta}+\Gamma\dot{\theta}+\frac{dU(\theta)}{d\theta}=0, \tag{1}$$

where J is the moment of inertia of the rotor, Γ represents a damping constant, and $U(\theta)$ stands for an orientation dependent Coulomb potential,

$$U(\theta)=\sum_{a,b}\frac{Kq_a^Rq_b^D}{|R_\alpha^R(\theta)-R_b^D|}, \tag{2}$$

where K is the Coulomb constant, q_a^R with $a\in\{\pm1\}$ denote the positive and negative charges on the two ends of the rotor dipole, and the vector $R_a^R(\theta)$ stands for their locations. By analogy, q_b^D with $b\in\{\pm n\}$, where $n=1,\ldots,N$, denotes the positive and negative charges on the two ends of the nth driver dipole and the vector $R_b^D(\theta)$ stands for their locations. On the complex plane, the vectors $R_a^R(\theta)$ and R_b^D are represented by the complex numbers

$$P_l^R(\theta)=r_re^{i(\theta+l\omega)}, \tag{3}$$

$$P_{jkl}^D=de^{i[2\pi(j-1)/N]}+r_de^{i[2\pi(j-1)/N+l\pi+w_k]},$$

where r_r (r_d) is the radius of the rotor (driver) and d denotes the distance between the rotor center and the driver center (Fig. 1). The indices $j\in\{1,2,\ldots,N\}$, $k\in\{1,2\}$, and $l\in\{0,1\}$, stand for the jth driver, its two conformational states, and their positive and negative charges, respectively.

When the conformations of the N drivers are fixed, the potential profile $U(\theta)$ of Eq. (1) is time independent. Under this profile, the rotor orientation θ will eventually be damped to a constant value, if $\Gamma\neq0$. But the stochastic ATP energy input changes the driver conformation respectively the potential $U(\theta)$ sequentially. Therefore, the long term behavior of θ will not stop at this value and is time dependent. The dynamics of θ is dominantly driven by the driver dipole closest to the rotor dipole through the Coulomb interaction. But it is damped by the resistance force Γ due to the surface contact between the rotor and all N drivers. Since the driving and damping forces belong to different kinds of interactions and come from different sources, the random force $dU(\theta)/d\theta$ in Eq. (1) need not follow the fluctuation-dissipation relation of the Brownian random forces in the conventional Langevin equation, even though these two equations look similar. Since the Brownian random force is assumed to be small compared with $dU(\theta)/d\theta$, it has been neglected in Eq. (1).

III. MOTOR EXAMPLES IN DIFFERENT SCALES

As an example, let us consider a micromachine approximately 3×10^3 times larger than F_0F_1ATPase. Since the length, the radius, and the weight of the central axis (γ subunit) in the F_0F_1ATPase are approximately 9.6 nm, 3.3 nm, and 12 218 atomic mass units (2.03×10^{-23} kg) [22], the radius R and weight M of the rotor in the micromachine are supposed to be 10^{-5} m and 10^{-12} kg, where M is proportional to R^3. Assume the nonuniformly distributed charge Q on the rotor is 10^{-18} C, which is approximately ten times larger than an electron charge 1.6×10^{-19} C. If the charges of the rotor and the drivers have a minimum distance $r_0\approx R$, the potential U is close to the order of $KQ^2/r_0\approx10^{-21}$ N m. The effective damping coefficient of the rotor along the rotated arc is estimated to be $C=10^{-12}$ kg s^{-1}=1 pN m^{-1} s^{-1}. Taking $\theta=0$ as a minimum of the potential $U(\theta)$ and $x=R\theta$ as the corresponding rotated arc, the behavior with which the rotor approaches the equilibrium position $x=0$ can be approximated by the equation

$$M\ddot{x}+C\dot{x}+Wx=0. \tag{4}$$

The coefficients in Eqs. (1) and (4) are related by $J=MR^2\approx10^{-22}$ kg m^2 and $\Gamma=CR^2\approx10^{-22}$ kg m^2 s^{-1}, and the potential well $U(\theta)$ around the minimum $\theta=0$ has been approximated by the quadratic curve $WR^2\theta^2/2$. The ATP energy is approximately 7.3 kcal/mole, corresponding to 5×10^{-20} J per ATP. Since the potential well $U(\theta)$ is created by one ATP, its energy WR^2 cannot be larger than the energy of an ATP molecule. In general, WR^2 can be much less than the ATP

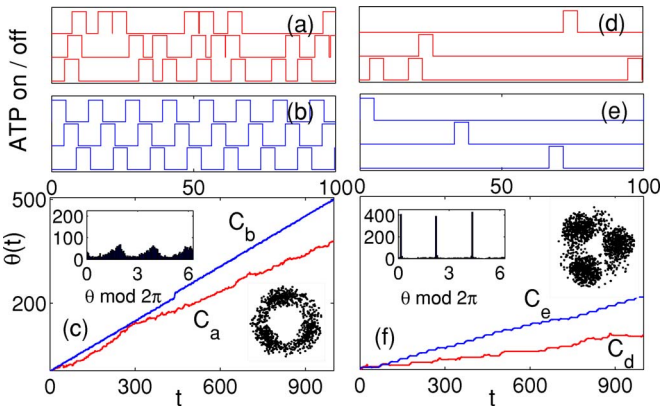

FIG. 2. (Color online) (a), (d) Random pulse sequences at three drivers for $\tau=5$ with $\tau^*=10$ and 500, respectively. (b), (e) Periodic pulse sequences for $\tau=5$ and pulse distance 8. (c), (f) The corresponding rotated angles $\theta(t)$ with orientation histograms and bead locations. (a), (b) [(d), (e)] correspond to high (low) ATP concentration. (The units depend on the motor sizes discussed in Sec. III.)

energy for two reasons: First, the driver dipoles and the rotor dipole are not overlapped. The larger the distance in between, the less the ATP energy on the driver is transported to the rotor. Second, so far the configurational change of the rotor is supposed to follow that of the drivers. It implies that the torque of the drivers is larger than that of the rotor or, equivalently, the energy difference between two driver conformations is larger than the energy difference between two rotor angles. However, even in the inefficient case that only 20% of the ATP energy is transported to the rotor, one has $W\approx 10^{-10}$ J.

Inserting above values into Eq. (4), the three terms in this equation are approximately of the order of 10^{-17}, 10^{-17}, and 10^{-15} N and the system is in the underdamped regime because $W/M>[C/(2M)]^2$. Equations (1) and (4) have the damping rate e^{-Gt} with $G=C/(2M)=\Gamma/(2J)$ and the speed $\dot{\theta}=\dot{x}/R$ derived from Eq. (4) can be solved explicitly [23]. Note that $\dot{\theta}$ is not the speed of rotation of the motor, but the speed with which it converges to a stable state after the conformations of the drivers are changed. The real rotational speed of the motor is determined by the ATP concentration or how frequently U is changed.

To keep the same C/M ratio between the first two terms in Eq. (4), the corresponding parameters in Eq. (1) can be selected as follows: $J=0.01$, $\Gamma=0.005$, $K=q_a^R=q_b^D=1$, $r_r=2$, $r_d=6$, $d=10$, $\omega=\pi/10$, $w_1=\pi/2$, and $w_2=\pi$. These dimensionless parameters with a small inertia, i.e., $J=0.01$, correspond to a microbiological system with a low Reynolds number. Even this J is not small enough to be in the overdamped regime; it is close to this regime, because the damping rate $e^{-Gt}=e^{-t/4}$ is fast. Within the period $t=12$ s of our environmental change in the example of the dense ATP pulses in Fig. 2(b), the damped ratio is $e^{-Gt}\approx 5\%$, which means the oscillation magnitude of θ has decreased 95%. That is, before the next energy packet is supplied, θ has almost arrived at its stable state. Therefore, the long term behavior of θ is not sensitive to whether the rest tiny oscillation is fast, slow, or overdamped. Consequently, the selected parameters lead to a similar unidirectional θ dynamics as that in the overdamped regime.

For a motor smaller than 10^{-5} m, the inertia term in Eq. (1) decreases faster than other two terms, since it is proportional to R^5. Accordingly, the system quickly goes beyond the boundary $W/M=(C/2M)^2$ into the overdamped regime. If the radius and the weight of the rotor are 10^{-8} m and 10^{-21} kg, i.e., only approximately three times larger than the F_0F_1ATPase, the three terms in Eq. (4) are of the order 10^{-29}, 10^{-20}, and 10^{-12} N. Therein the value of C has been supposed to be the same as before. Even though C varies with R, it cannot decreases as fast as R^5 as does the inertia term. Therefore decreasing motor size leads to more apparent unidirectional motion of θ. On the other hand, if the motor is larger than 3×10^3 times the F_0F_1ATPase, the inertia term becomes significant. But its averaged rotational motion still can be unidirectional. Only the fluctuation around this averaged motion will become larger. Consequently the idea of the DRM discussed here can also be applied to drive macroscale systems with a larger inertia, for which the term J in Eq. (1) is not negligible.

After an ATP releases energy to a driver, the driver stays at a high energy state for a period τ, which can be stochastic [Figs. 2(a) and 2(d)] or periodic [Figs. 2(b) and 2(e)]. In the former case, the distance between two neighbor pulses is distributed as $-\tau^* \ln(R)$ with a positive factor τ^* and a random value $R\in[0,1]$. The curves C_a, C_b, C_d, and C_e in Figs. 2(c) and 2(f) depict the rotor angles θ in time under the driving pulses (a), (b), (d), and (e). All these curves have positive slope, which tells us that the rotor rotates unidirectionally, no matter whether the ATP pulses (energy supply) are periodic or random. Second, C_b is steeper than C_a and C_e is steeper than C_d. It indicates that if the averaged densities of ATP pulses are the same [as in (a) and (b)), then a periodic energy supply is more efficient than a random energy supply. Furthermore, C_a is steeper than C_d and C_b is steeper than C_e. This reveals that the denser the driving pulses (energy), the faster the rotation. The histograms of the rotor orientation θ for the (a) and (d) pulses are presented in the upper insets of (c) and (f), which shows that the orientation is more uniformly distributed for dense sequences but sharply localized like δ peaks for dilute sequences. Let us attach a bead to the rotor acentrically to characterize the rotor orientation θ and allow the bead to fluctuate slightly in both rotational and radical directions. After randomizing the orientation θ in C_b and C_e slightly combined with a small fluctuation in the radical direction, one obtains the cloudy ring patterns for the bead location in (c) and (f), which resemble the orientation distribution of the γ subunit in the F_0F_1ATPase experiment with high respectively low ATP concentrations [24,25]. The cloudy patterns together with the histograms reveal that the rotor dipole has a more uniform orientation distribution if the energy supply is dense. In contrast, the orientation of this dipole is more localized at three angles if the energy supply is dilute.

To demonstrate the rotation efficiency in different rotor and driver configurations, Fig. 3 shows the rotated angle θ versus the relative rotor radius $\rho_r=r_r/d$ and the relative distance $\rho_e=e/d$, with the border distance $e=d-r_r-r_d$ (see Fig. 1), where the center distance d is kept constant. The angle θ

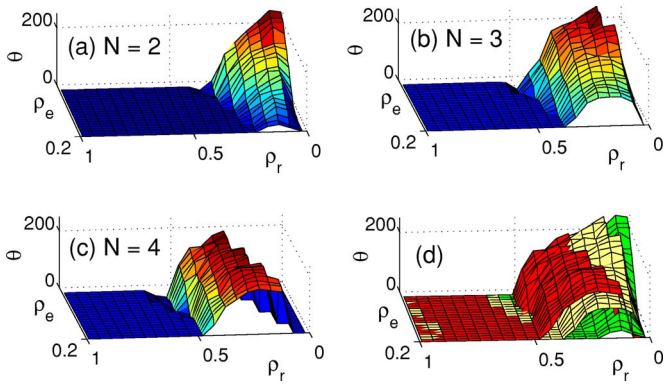

FIG. 3. (Color online) The rotation efficiencies for different driver and rotor configurations with $N=2$, 3, and 4 in green, yellow, and red.

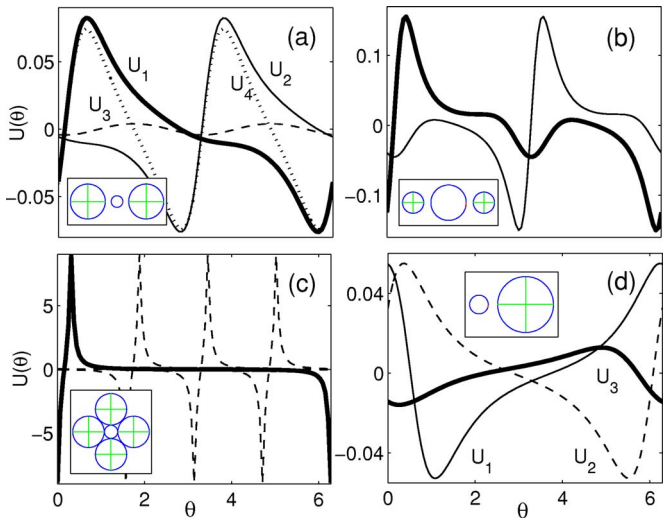

FIG. 4. (Color online) Ratchet potentials for different rotor and driver configurations in the inset with $d=10$ and $(N,\rho_r,\rho_e)=(2,0.2,0.2)$, (2, 0.5, 0.2), $(4,1-\sqrt{2}/2,0.01)$, and (1, 0.2, 0.2) in (a), (b), (c), and (d) respectively. (The units depend on the motor sizes discussed in Sec. III.)

is assigned to zero at the (ρ_d,ρ_e) plane if the corresponding drivers are too large to overlap each other and forbidden. For the one driver case with $N=1$, there is no directional rotation. For $N=2$, 3, and 4 with $\Gamma=0.05$, the directional rotated angle θ is plotted in Fig. 3 after approximately 80 ATP's have been hydrolyzed by each driver [80 pulses in each sequence in Fig. 2(a)]. A comparison shows that the larger the number N, the faster the rotation of the rotor will be, up to the exception in the small (ρ_r,ρ_e) region. In this region the drivers are too large to overlap each other and the corresponding configuration is physically forbidden. Therefore, a comparison there is meaningless. The plot in Fig. 3 indicates that the directional rotation is faster in the small ρ_e regime, e.g., [0, 0.2], corresponding to a close distance between rotor and drivers, and in the small ρ_r regime, e.g., [0.1, 0.4], which will become clear after the following investigation on the system potential $U(\theta)$.

It should be recalled that the current model is under the assumption that the torque of the drivers is much larger than the torque of the rotor. The advantage of this assumption is that it helps us easily realize why the motor works. Once we understand this simple model, the directional rotation in more general models, where the transition constants are dependent on the rotor positions, would not be so surprising. Notably, ATP energy is just an example in the current model and can be replaced by other energy sources.

IV. SPATIAL AND TEMPORAL SYMMETRY BREAKING

For $N=2$ the potential U_1 (thick solid) and U_2 (thin solid) in Fig. 4(a) correspond to the cases where only the first or the second driver, respectively, is at the high energy state w_2. The potential U_3 (dashed) and U_4 (dotted) correspond to the case when both drivers are respectively at low and high energy states. Although the asymmetric potential profiles of U_1, U_2, and U_4 are similar to that in the flashing ratchet proposed for the muscle contraction [4], their functions are different. The flashing ratchet contains a flat potential and a periodic asymmetric potential. The asymmetric potential and the noise are two globally unbiased driving sources which can only shift the particles locally. Switching between these two sources leads to biased particle motion, in agreement with the concept of Parrondo's paradox [26]. In the current DRM, e.g., with $N=2$, the previous noise is replaced by another asymmetric potential U_2 which is almost the same as U_1 up to a phase shift π [Fig. 4(a)]. The driving by U_2 is more efficient than the noise since U_2 moves the particle in the same biased direction as U_1 does, while the noise spreads out the particles uniformly in both directions and reduces the efficiency of their biased movement. Under proper switching frequency, the vibrating ratchet in Fig. 4(a) can be as efficient as wave surfing, in which the surfer always stands in front of the wave front and is carried forward as fast as a moving wave [27]. Accordingly, such surfing ratchet is in general more efficient than a flashing ratchet [28].

Figure 4(b) has a larger rotor and two smaller drivers but with the same distance d, which forms a secondary potential minimum around $\theta=3$ to trap the θ state. It explains the general efficiency decrease in Fig. 3 when the rotor size is too large, e.g., $\rho_r>0.3$. For $N=3$, the potential peaks are similar to Fig. 4(a) but with a shorter phase shift, $2\pi/3$, between them. Figure 4(c) depicts the sharp potentials from four densely located drivers. Note that the asymmetric potentials in Fig. 4 are due to the asymmetric location of the *rotor* dipole, from which the name *dipole ratchet* derives. If this dipole is centered at the origin, the directional rotation will not occur. It cannot be rescued by any asymmetric locations of the driver dipoles.

For a one driver system, $N=1$, a directed rotation will not happen, regardless of which two conformational states w_1 and w_2 are selected for the driver. The reason is clear from the example in Fig. 4(d) showing that a state θ cannot escape from the region $[0,2\pi]$ by switching between two potentials $U_1(w_1=-\pi/12)$ and $U_2(w_2=13\pi/12)$, because the two corresponding attractors in the phase space of these two potentials have approximately the same basin, which is bounded by $[0,2\pi]$ in the θ coordinate. In this case, the rotor and the driver resemble two connected sawtooth wheels. If a wheel

(dipole) vibrates back and forth, the other cannot rotate unidirectionally.

Although a directional rotation for $N=1$ cannot be created by a spatial symmetric breaking, it can be induced by a temporal symmetry breaking. Indeed, suppose the driver has three conformational states with orientations w_1, w_2, and w_3 and arrives at the high energy state w_2 directly after ATP hydrolysis but returns to the low energy state w_1 through a metastable middle energy state w_3 and stays there for a while. Then the dynamics of the driver orientation follows the specified temporal sequence "low, high, middle energy states" repeatedly. This specifies a time arrow for visiting these three states and leads to rotation. As an example, let us take $w_3=3\pi/12$ as the orientation of the metastable state, which creates the potential U_3 in Fig. 4(d). Clearly, on repeating driving the system by the sequence $U_1,U_2,U_3,U_1,U_2,U_3,\ldots$, a state θ tends to move from a potential minimum to another potential minimum rightward. Note that this happens even when the potentials are spatially symmetric. This result indicates that the minimal driver conformation number for a unidirectional rotation for $N=1$ is three. It is consistent with the fact that three is the least position number on a circle that can specify a rotation direction.

V. DISCUSSION

As mentioned at the beginning, the ratchet model has been used to describe huge number of different biased motions. The core ingredient in this model is a point on an asymmetric potential under a specific driving force. This point usually represents the coordinate of an object in the real space [1,2,4–9]. However, it also can represent a physical state in a generalized state space. In this case the asymmetric potential in the state space is not necessarily related to whether the potential in the real space is asymmetric or not. The orientation θ of the rotor in the DRM is an example. The asymmetric potentials in Fig. 4 (state space) come from the asymmetric location of the rotor dipole and are not directly related to the symmetry and periodicity of the pulse potential of ATP in Figs. 2(a), 2(b), 2(d), and 2(e) (real space). This fact indicates an extension possibility of the ratchet concept to different generalized state spaces.

Dipole effect has been found to play a significant role in the function of the ion pump Na,K-ATPase [21]. Experiments showed that this motor can transport ions through the cell membrane under an oscillating electric field [5]. It indicates a non-negligible large scale dipole inside the pump besides the small scale peptide dipoles. A theoretical dipole model on this motor called the theory of electroconformational coupling [5] has reproduced experimental results on ion transport [5] and on stochastic resonance [29–32]. These results confirm the significant role of a dipole force in the function of the molecular motors.

According to the chemiosmotic hypothesis, ATP synthesis in mitochondria is by the transduction of electrochemical potential energy through the action of F_0F_1ATPase. When the transmembrane proton concentration gradient is sufficiently large, the proton flux through the F_0 subunit drives the central γ axis to rotate. Since γ is not centrally symmetric, its rotation applies power strokes to the three surrounding β subunits in a clockwise time sequence [20]. These sequential conformational changes of the β's induce ATP synthesis on them. However, if the transmembrane proton gradient is low and the ATP concentration is high, ATP can instead hydrolyze and fuel β's to rotate γ in opposite direction. While the ATP bombardment on each β is stochastic, its docking and hydrolysis on each β are found to follow a counterclockwise time sequence, indicating a sophisticated structure correlation between these three separated β subunits. Interestingly, as shown in Figs. 2(c) and 2(f), such correlation is not a necessary condition for a unidirectional rotation and the efficiency from uncorrelated driving is not much smaller than a correlated driving if the ATP is densely fueled. Nature seems to select a much complex, but optimally efficient, model for the rotary motor in our cell.

In summary, this work demonstrates the feasibility of rotating a dipole by fluctuating its ambient dipoles. The requirement for this directional motion is temporal symmetry breaking for one driver systems and spatial symmetry breaking for multidriver systems. The present result is not only valid for microsystems fueled by ATP but also applicable to macrosystems under general fluctuating sources.

ACKNOWLEDGMENTS

The authors would like to thank Dr. Nan-Yow Chen for his numerical estimation of the internal energy and the dipoles of F_0F_1ATPase in different conformations based on the F_1ATPase x-ray structure in the Protein Data Bank. This work has been financially supported by the National Science Council at Taiwan under Contract No. 94-2112-M-009-025.

[1] R. D. Astumian, Science **276**, 917 (1997).
[2] P. Reimann, Phys. Rep. **361**, 57 (2002).
[3] R. D. Astumian and I. Derenyi, Eur. Biophys. J. **27**, 474 (1998).
[4] F. Jüdlicher, A. Ajdari, and J. Prost, Rev. Mod. Phys. **69**, 1269 (1997).
[5] T. Y. Tsong and R. D. Astumian, Bioelectrochem. Bioenerg. **15**, 457 (1986); T. Y. Tsong and R. D. Astumian, Prog. Biophys. Mol. Biol. **50**, 1 (1987); T. D. Xie, P. Marszalek, Y.-D. Chen, and T. Y. Tsong, Biophys. J. **67**, 1247 (1994); T. D. Xie, Y.-D. Chen, P. Marszalek, and T. Y. Tsong, *ibid.* **72**, 2496 (1997).
[6] D. E. Feldman, S. Scheidl, and V. M. Vinokur, Phys. Rev. Lett. **94**, 186809 (2005).
[7] D. E. Shalóm and H. Pastoriza, Phys. Rev. Lett. **94**, 177001 (2005).
[8] E. Lundh and M. Wallin, Phys. Rev. Lett. **94**, 110603 (2005).
[9] B. Y. Zhu, F. Marchesoni, and F. Nori, Phys. Rev. Lett. **92**,

180602 (2004).
[10] F. Alonso-Marroquin and H. J. Herrmann, Phys. Rev. Lett. **92**, 054301 (2004).
[11] D. van der Meer, P. Reimann, K. van der Weele, and D. Lohse, Phys. Rev. Lett. **92**, 184301 (2004).
[12] M. v. Smoluchowski, Phys. Z. **13**, 1069 (1912).
[13] R. P. Feynman, *The Feynman Lectures on Physics*, (Addison-Wesley, Massachusetts, 1963), Vol. 1, Chap. 46.
[14] E. B. Stukalin, Hubert Phillips III, and A. B. Kolomeisky, Phys. Rev. Lett. **94**, 238101 (2005).
[15] R. Golestanian, T. B. Liverpool, and A. Ajdari, Phys. Rev. Lett. **94**, 220801 (2005).
[16] P. Thomen, P. J. Lopez, and F. Heslot, Phys. Rev. Lett. **94**, 128102 (2005).
[17] H. Goko and A. Igarashi, Phys. Rev. E **71**, 061108 (2005).
[18] Y. Kafri, D. K. Lubensky, and D. R. Nelson, Phys. Rev. E **71**, 041906 (2005).
[19] A. Mogilner, H. Wang, T. Elston, and G. Oster, in *Computational Cell Biology*, edited by C. Fall, E. Marland, J. Wagner, and J. Tyson (Springer-Verlag, New York, 2002).
[20] H. Wang and G. Oster, Nature (London) **396**, 279 (1998).
[21] L. Stryer, *Biochemistry*, 4th ed. (Freeman & Co. New York, 1995).
[22] These values are determined from the Protein Data Bank.
[23] In the regime of damped oscillation $W/M > (C/2M)^2$, the solution of Eq. (4) is $x(t)=Ae^{-Gt}\sin(\omega t+\phi_0)$ where $A=\sqrt{x_0^2+\{[(C/2M)x_0+\dot{x}_0]/\omega\}^2}$ and $\phi_0=\tan^{-1}\{x_0\omega/[(C/2M)x_0+\dot{x}_0]\}$ are determined by the initial conditions and $\omega=\sqrt{W/M-(C/2M)^2}$. For details see general textbooks of differential equations.
[24] R. Yasuda, H. Noji, K. Kinosita, Jr., and M. Yoshida, Cell **93**, 1117 (1998).
[25] K. Adachi, R. Yasuda, H. Noji, H. Itoh, Y. Harada, M. Yoshida, and K. Kinosita, Jr., Proc. Natl. Acad. Sci. U.S.A. **97**, 7243 (2000).
[26] G. P. Harmer and D. Abbott, Nature (London) **402**, 864 (1999); C.-H. Chang and T. Y. Tsong, Phys. Rev. E **67**, 025101(R) (2003).
[27] T. Y. Tsong and C.-H. Chang, AAPPS Bull. **13**(2), 12 (2003); T. Y. Tsong and C.-H. Chang, Physica A **350**, 108 (2005).
[28] A. Parmeggiani, F. Jülicher, A. Ajdari, and J. Prost, Phys. Rev. E **60**, 2127 (1999).
[29] C.-H. Chang and T. Y. Tsong, Phys. Rev. E **69**, 021914 (2004).
[30] I. Goychuk and P. Hänggi, Phys. Rev. Lett. **91**, 070601 (2003).
[31] L. Gammaitoni, P. Hänggi, P. Jung, and F. Marchesoni, Rev. Mod. Phys. **70**, 223 (1998).
[32] A. Fuliński, Phys. Rev. Lett. **79**, 4926 (1997).